Numerical Analysis of Magnetohydrodynamics Flow in a Curved Duct

Md. Mainul Hoque, Nisat Nowroz Anika and Md. Mahmud Alam

Abstract— The effects of a transverse magnetic field on the steady motion of a conducting, viscous and incompressible fluid through a curved duct of circular cross section is studied in this paper. The curvature of the duct has been assumed to be small, that is, the radius of the circle in which the central line of the duct is coiled is large in comparison with the radius of the cross section. A solution is developed by Spectral method is applied as a main tool for the numerical technique; where, Fourier series, Chebyshev polynomials, Collocation methods, and Iteration method are used as secondary tools. The dimensionless parameters of the problem are Dean number (D_n) and magnetic parameter (M_g). Two vortex solutions have been found. Axial velocity has been found to increase with the increase of Dean number, while decrease with the increase of curvature and magnetic parameter. For high magnetic parameter & Dean number and low curvature almost all the fluid particles strength are week. The axial velocity contours are shown to be shifted toward the outer wall. Due to the combined effect of the magnetic field and Dean number a bracelet has been originates from the right corner of the duct and expands for high Dean number and curvature.

Index Terms— Transverse Magnetic field, Dean Number, Curvature, Spectral Method.

1 INTRODUCTION

FULLY developed flow in curved ducts is encountered in various practical processes. In the analysis of fluidic devices, flows in separation processes, heat exchangers, physiological systems are examples of such processes. In the past few decades, most of the research works have been done on the fully developed flow through curved ducts. Therefore, the fully developed flow phenomena in the curved ducts have drawn a keen attention.

Dean (1927) first formulated the curved duct problem mathematically under the fully developed flow conditions and confirmed the existence of a pair of counter rotating vortices as a secondary flow in the curved duct. For the fully developed flow in a curved circular duct, Ito (1951) and Cuming (1952) separately showed the existence of a two-vortex secondary flow patterns by using perturbation method as was done by Dean (1927). McConalogue and Srivastava (1968) obtained numerical solutions for fully developed flow through a curved duct for the range of $96 < D_n \le 600$ by expanding in Fourier series and then integrating the resulting ordinary differential equations numerically.

Cheng and Akiyama (1970) and Cheng et al. (1975) reported two-vortex secondary flow patterns in a curved duct with square cross-section by using finite difference method. Masliyah (1980) investigated both numerically and experimentally the flow through a semi-circular duct with a flat outer wall. Both Nandakumar and Masliyah (1982) and Dennis and Ng (1982) separately obtained dual solution for the flow through a curved tube with circular cross-section. Later, the stability of the dual solutions of two-vortex and four-vortex secondary flow patterns was studied by Yanase et al. (1989). They found that the two-vortex secondary flow patterns are stable while the four-vortex flow patterns are unstable. In the numerical research works by Shanthini and Nandakumar (1986), Winters (1987) and Daskopolous and Lenhoff (1989), dual solutions for fully developed flow in a curved duct of square cross-section are found. Winters also found that there are many symmetric and asymmetric solutions, although many of them are linearly unstable.

In the early work, the four-vortex secondary flow patterns were found with two minor weak vortices. These two minor weak vortices are generated near the outer wall of the duct cross-section. Both Cheng and Akiyama (1970) and Cheng et al. (1975) found two-vortex secondary flow patterns for square cross-section by applying finite difference method. But Joseph et al. (1975), Ghia and Sokhey (1977) and De Vriend (1981) found four-vortex secondary flow patterns for rectangular cross-section of the duct. Cheng et al. (1977) investigated the flow patterns in curved rectangular channel for finite and infinite aspect ratios of the cross-section and analyzed the flow field in a fully developed laminar flow.

Recently, Mainul et.al (2013) investigates the effects of magnetic field in the curved duct for curvature 0.2. In the present work our aim is to obtain a detail results on the Dean numbers as well as magnetic parameter at curvatures $\delta = 0.5$. In this present study, the magnetic field has been imposed along the center line of a curved duct.

- *Md. Mainul Hoque, is currently pursuing PhD degree in Chemical engineering from The University of Newcatle, Australia, PH-+6140681412. E-mail: pavel.math.ku@gmail.com*
- *Nisat Nowroz Anika is currently pursuing masters degree program in Applied Mathematics in Khulna University, Bangladesh, PH-+8801753359538. E-mail:anikamathku07@gmail.com*
- *Md. Mahmud Alam, is a Professor, Mathematics Discipline, Khulna University, Bangladesh, PH-+8801912982811. E-mail: alam_mahmud2000@yahoo.com*

2 Problem Formulation

Let us consider a curved duct with circular cross-section containing incompressible inviscid fluid (Figure: 1). Let the radius of the duct be L, radius of cross-section be a. To reach the point (x,y,z) we have to travel $L+r$ unit ($0 \le r \le a$) along x-axis, then turn an angle θ considering the origin as centre in the xy plane, then turn again an angle α in the plane of cross-section. Then (x,y,z) and (r,α,θ) are related as,

$$x=(L+r\cos\alpha)\cos\theta,\ y=(L+r\cos\alpha)\sin\theta,\ z=r\sin\alpha$$

2.1 Basic Equations

For incompressible fluid, the equation of motion

$$\frac{dq}{dt}=F-\frac{1}{\rho}\nabla p+\nu\nabla^2 q \tag{1}$$

Here,

$$\frac{dq}{dt}=\frac{\partial q}{\partial t}+(q.\nabla)q \tag{2}$$

Then equation (1) becomes

$$\frac{\partial q}{\partial t}+(q.\nabla)q=F-\frac{1}{\rho}\nabla p+\nu\nabla^2 q \tag{3}$$

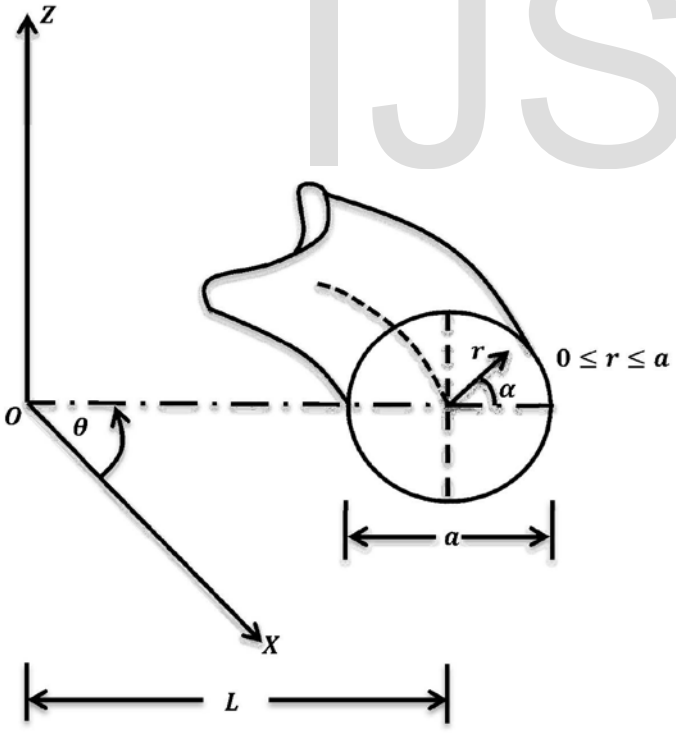

Figure. 1: Toroidal Coordinate systems for curved duct with magnetic field

Since, a magnetic field of constant strength is imposed to act throught perpendicular to the central axis of the curved duct in the direction of Z- axis as shown in the figure-1. Since the velocity field is modified by the magnetic field vector and the equation of motion appears a body force $\frac{1}{\rho}J\wedge B$ per unit volume of electro- magnetic origin. If there is no other body force then the equation of motion (3) becomes

$$\frac{\partial q}{\partial t}+(q.\nabla)q=-\frac{1}{\rho}\nabla p+\nu\nabla^2 q+\frac{1}{\rho}J\wedge B \tag{4}$$

2.2 Toroidal Coordinates System

Let us defined the following non-dimensional variables

$$u'=\frac{q_r}{\frac{\upsilon}{a}}\quad v'=\frac{q_\alpha}{\frac{\upsilon}{a}}\quad w'=\frac{q_\theta}{\frac{\upsilon}{a}}\sqrt{\frac{2a}{L}}\quad r'=\frac{r}{a}$$

$$S'=\frac{L\theta}{a}\quad \frac{a}{L}=\delta\quad p'=\frac{p}{\rho\left(\frac{\upsilon}{a}\right)^2}$$

where u',v',w' are non-dimensional velocities along the radial, circumferential and axial direction respectively. r' is non-dimensional radius, S' is the non-dimensional axial variable, δ is non-dimensional curvature and p' non-dimensional pressure.

Non-dimensional continuity equation:

$$r'(L+ar'\cos\alpha)\frac{\partial u'}{a\partial r'}+\frac{(L+ar'\cos\alpha)u'}{a}+r'(u'\cos\alpha-v'\sin\alpha)+r'\sqrt{\frac{L}{2a}}\frac{\partial w'}{\partial\theta}=0 \tag{5}$$

Non-dimensional radial momentum equation:

$$u'\frac{\partial u'}{\partial r'}+\frac{v'}{r'}\frac{\partial u'}{\partial\alpha}-\frac{v'^2}{r'}-\frac{Lw'^2\cos\alpha}{2(L+ar'\cos\alpha)}=-\frac{\partial p'}{\partial r'}-\frac{\partial}{r'\partial\alpha}\left(\frac{\partial v'}{\partial r'}+\frac{v'}{r'}-\frac{\partial u'}{r'\partial\alpha}\right)-\sigma'\mu_e a^2 u' H_\theta^2 \tag{6}$$

Non-dimensional circumferential momentum equation:

$$r'u'\frac{\partial v'}{\partial r'}+\frac{v'}{r'}\frac{\partial v'}{\partial\alpha}+u'v'+\frac{Lr'\sin\alpha}{2(L+ar'\cos\alpha)}w'^2=-\frac{\partial p'}{\partial\alpha}+r'\frac{\partial}{\partial r'}\left(\frac{\partial v'}{\partial r'}+\frac{v'}{r'}-\frac{\partial u'}{r'\partial\alpha}\right)-\sigma'\mu_e a^2 v' H_\theta^2 \tag{7}$$

Non-dimensional axial momentum equation:

$$\left(u'\frac{\partial}{\partial r'}+\frac{v'}{r'}\frac{\partial}{\partial\alpha}\right)w'+\frac{a\cos\alpha}{L+ar'\cos\alpha}u'w'-\frac{a\sin\alpha}{L+ar'\cos\alpha}v'w'=-\frac{1}{L+ar'\cos\alpha}\frac{a^3}{\rho\upsilon^2}\sqrt{\frac{2a}{L}}\frac{\partial p}{\partial\theta}$$

$$+\left\{\left(\frac{1}{r'}+\frac{\partial}{\partial r'}\right)\frac{\partial w'}{\partial r'}+\left(\frac{1}{r'}+\frac{\partial}{\partial r'}\right)\frac{aw'\cos\alpha}{L+ar'\cos\alpha}+\frac{1}{r'^2}\frac{\partial^2 w'}{\partial\alpha^2}-\frac{a\partial}{r'\partial\alpha}\left\{\frac{w'\sin\alpha}{L+ar'\cos\alpha}\right\}\right\} \quad (8)$$

The other variables without primes are dimensional variables. Constant pressure gradient force is applied along the axial direction through the centre of cross section.

With the help of the above dimensionless variables and the boundary conditions the equation of motion reduces to the following form:

$$\frac{1}{r'}\left\{\frac{\partial\psi}{\partial r'}\frac{\partial(\Delta\psi)}{\partial\alpha}-\frac{\partial\psi}{\partial\alpha}\frac{\partial(\Delta\psi)}{\partial r'}\right\}+\Delta^2\psi+w'\left(\sin\alpha\frac{\partial w'}{\partial r'}+\frac{\cos\alpha}{r'}\frac{\partial w'}{\partial\alpha}\right)-M_g\Delta\psi=0 \quad (9)$$

and $$\frac{1}{r'}\left(\frac{\partial\psi}{\partial r'}\frac{\partial w'}{\partial\alpha}-\frac{\partial\psi}{\partial\alpha}\frac{\partial w'}{\partial r'}\right)+\Delta w'+D_n=0 \quad (10)$$

Here, ψ is the stream function defined by, $u'=\frac{1}{r'}\frac{\partial\psi}{\partial\alpha}$, $v'=-\frac{\partial\psi}{\partial r'}$, G is the constant pressure gradient force, μ is the viscosity, υ is the kinematic viscosity, D_n is the Dean number and M_g is the magnetic parameter. Equation (9) and (10) are called secondary and axial flow respectively.

where, $\Delta\equiv\frac{\partial^2}{\partial r'^2}+\frac{1}{r'}\frac{\partial}{\partial r'}+\frac{1}{r'^2}\frac{\partial^2}{\partial\alpha^2}$,

$$\Delta^2\equiv\frac{\partial^4}{\partial r'^4}+\frac{2}{r'}\frac{\partial^3}{\partial r'^3}-\frac{1}{r'^2}\frac{\partial^2}{\partial r'^2}+\frac{2}{r'^2}\frac{\partial^4}{\partial r'^2\partial\alpha^2}+\frac{1}{r'^3}\frac{\partial}{\partial r}-\frac{2}{r^3}\frac{\partial^3}{\partial r'\partial\alpha^2}+\frac{4}{r'^4}\frac{\partial^2}{\partial\alpha^2}+\frac{1}{r'^4}\frac{\partial^4}{\partial\alpha^4}$$

$G=-\frac{\partial p}{\partial S}$, $D_n=\frac{a^3}{\mu\upsilon}\sqrt{\frac{2a}{L}}G$ and $M_g=\sigma'\mu_e a^2H_\theta^2$.

3 Numerical Technique

This study depends on the Magnetohydrodynamics Navier-Stokes momentum equation. When the flow is driven only by pressure gradient force parabolic velocity profile is found. But, when the flow is subjected to magnetic field and curvature the Magnetohydrodynamics Navier-Stokes equation become non-linear. It becomes very difficult to solve the equations analitically. For obtaining the solution of such problems we adopt advanced numerical methods. The governing equations of our problem contain a system of partial differrential equations which will be transformed by usual transformation into a non-dimensional system of non-linear partial differential equations with boundary conditions. Usually the theoretical treatment of flow in a curved duct has been made either analytically or numerically. The present work is mainly based on numerical methods. For this purpose the Spectral method has been used to solve the equations. As for the spectral collocation method (Gottlieb and Orszag, 1977) which will be mainly used in this dissertation, it is necessary to discuss the method in brief. The expansion by polynomial functions is utilized to obtain steady or non-steady solution. Fourier series and Chebyshev polynomials are used in circumferential and radial directions respectively. Assuming that steady solution is symmetric with respect to the horizontal line of the cross-section, ψ and w' are expanded as,

$$\psi(r',\alpha)=\sum_{n=1}^{N}f_n^s(r')\sin n\alpha+\sum_{n=0}^{N}f_n^c(r')\cos n\alpha$$

and $$w'(r',\alpha)=\sum_{n=1}^{N}w_n^s(r')\sin n\alpha+\sum_{n=0}^{N}w_n^c(r')\cos n\alpha$$

where, N is the truncation number of the Fourier series. The collocation points are taken to be, $R=\cos\left\{\frac{N+2-i}{N+2}\right\}\pi\ [1\le i\le N+1]$. Then we get non-linear equations for $W_{nm}^s, W_{nm}^c, F_{nm}^s, F_{nm}^c$. The obtained non-linear algebraic equations are solved under by an iteration method with under-relaxation.

Convergence of this solution is taken up to five decimal places by taking $\varepsilon_p<10^{-5}$. Here, p is the iteration number. The values of M and N are taken to be 60 and 35 respectively for better accuracy. Where,

$$\varepsilon_p=\sum_{n=1}^{N}\sum_{m=0}^{M}\left[\left(F_{mn}^{s(p)}-F_{mn}^{s(p+1)}\right)^2+\left(W_{mn}^{s(p)}-W_{mn}^{s(p+1)}\right)^2\right]+\sum_{n=0}^{N}\sum_{m=0}^{M}\left[\left(F_{mn}^{c(p)}-F_{mn}^{c(p+1)}\right)^2+\left(W_{mn}^{c(p)}-W_{mn}^{c(p+1)}\right)^2\right]$$

4 Results And Discussions

Flow through a curved duct of circular cross section with Magnetic parameter has been considered. The flow is governed by three non dimensional parameters: the Dean number (D_n), curvature (δ) and the magnetic parameter (M_g). The main flow is forced by the magnetic field as well as pressure gradient along the centre line of the duct. For circular cross sectional duct, steady solution has been obtained by using the spectral method where Chebyshev polynomials and Fourier series have been used in the radial and circumferential direction respectively.

At the outset, the calculation for steady laminar flow for viscous incompressible fluid has been analyzed under the action

of Dean number as well as magnetic parameter at curvatures $\delta = 0.5$.

The results have been shown through stream line, vector plots of the secondary flow and contour plots of the axial flow. In both the cases, inner side is to the left and outer side is to the right. The arrows in the vector plots (Figs. 2-9) denote the direction and magnitude of the secondary velocity. In case of contour plots (Figs. 2-9) the distance between two consecutive contours is adjusted automatically and kept invariant throughout this dissertation. The stream line, vector and contour plots of the flow development have been shown at different magnetic parameters which are arranged in a column form left to right. In each figure, three columns have been produced. Among them the left column shows the stream line, middle and right column shows, vector plots of the secondary flow and contour plots of the axial flow behaviors in that order. The obtained results are stated below. Six cases have been considered as:

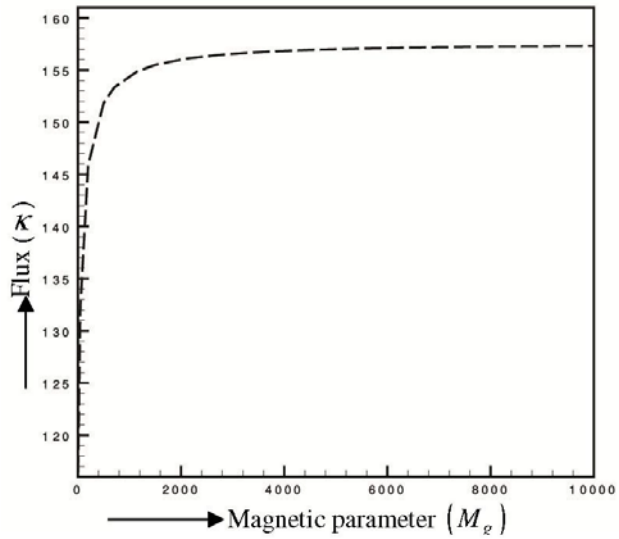

Flux (κ)

4.1 Dean number (D_n) = 400 at Curvature (δ) = 0.5

After a comprehensive survey over the parametric space, steady solution curve has been obtained in Fig. 2 for non-dimensional flux (κ) with the variation of magnetic parameter for $D_n = 400$ and $\delta = 0.5$. For each figure the total flow is found to decreases as the magnetic parameter increase. The highest flux is found at $\delta = 0.5$ and $M_g = 10000$. The flow structures has been depict at the several points of (M_g) in Fig. 2 when $\delta = 0.5$.

The difference of the stream line, vector plots of the secondary flow and axial flow for different values of magnetic parameter have been discussed for Dean Number $D_n = 400$. In Fig. 3 the stream line, vector plots of the secondary flow and axial flow for different values of magnetic parameter at Dean Number $D_n = 400$ have been shown at the first, second and third column respectively. The highest value of magnetic parameter, increment in axial velocity (Δw), increment in constant $\psi -$ lines ($\Delta\psi$) have been given on the right side. For each figure the outer wall is to the right and the inner wall is to the left.

The length of arrow indicates the ratio of the stream velocity to the axial velocity and the direction of the flow in vector plots are always indicates by an arrowhead, no matter how small the flow is. Thus, the relative strength of the flow is not resolved for areas of a very weak secondary flow.

In Fig. 3 the vector plots of the secondary flow show the direction of the fluid particles and the strength of the vortex is shifted towards outer half of the cross-section as magnetic parameter increases. Velocities of the particles above the centre again increase due to the magnetic effect at $M_g = 3300$, but the velocity of the particles below the centre of cross–section keeps decreasing.

Finally two vortex flow is found where the upper vortex is rotating anti–clock wise and the lower vortex is rotating clock wise, but the strength of the two vortices are almost same. At $M_g = 6000$ and $D_n = 400$ axial flow contours are nearly circular and are eccentric with the centers shifted towards the inner wall of the tube duct as a result almost all the fluid particles strength are week. In that case almost all the fluid particle is shifted to the centre from the wall of the cross section as magnetic parameter increases.

4.2 Dean number (D_n) = 800 at Curvature (δ) = 0.5

In Fig. 4 non-dimensional flux (κ) has been plotted against magnetic parameter for $D_n = 800$ and $\delta = 0.5$. And it is clear that the flux increases with the increase of magnetic parameter. But if the magnetic parameter increases continuously the rate of change flux is negligible. For each figure the total flow is found to decreases as the magnetic parameter increase. The highest flux is found at $\delta = 0.5$ and $M_g = 15000$. For $M_g > 15000$ and $\delta = 0.5$ convergence criteria is very poor and as a result stable solution has not been found beyond this region. The stable solution zone initially increases with the increase of curvature. The largest magnetic parameter to give stable solution is $M_g = 11500$ for $\delta = 0.5$.

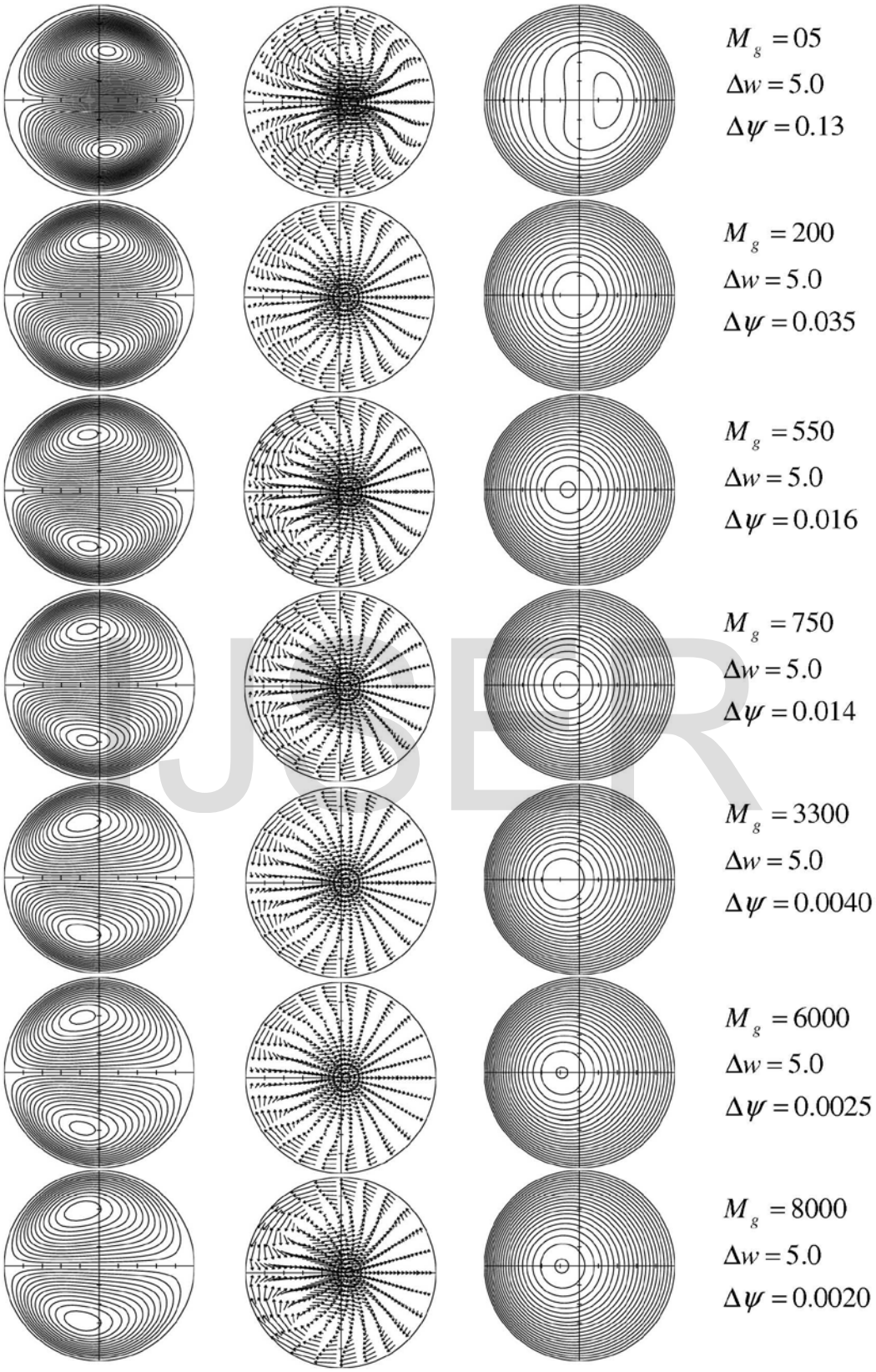

Fig. 3: The secondary flow, vector plots of the secondary flow and axial flow for different values of magnetic parameter at Dean Number $D_n = 400$

In Fig. 6 the stream line, vector plots of the secondary flow and axial flow for different values of magnetic parameter at Dean Number $D_n = 800$ have been shown at the first, second and third column respectively.

The highest value of magnetic parameter, increment in axial velocity (Δw), increment in constant $\psi -$ lines ($\Delta\psi$) have been given on the right side of the above figures. For each figure the outer wall is to the right and the inner wall is to the left. The length of arrow indicates the ratio of the stream velocity to the axial velocity and the direction of the flow in vector plots are always indicates by an arrowhead, no matter how small the flow is. Thus, the relative strength of the flow is not resolved for areas of a very weak secondary flow. In Fig. 6 the vector plots of the secondary flow show the direction of the fluid particles and the strength of the vortex is shifted towards outer half of the cross-section as magnetic parameter increases.

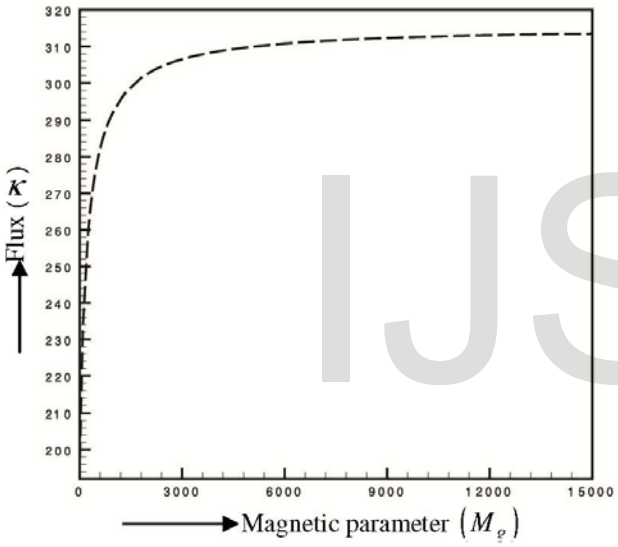

Fig. 4: Flux κ versus magnetic parameter M_g for Dean number $D_n = 800$

In case of secondary flow behavior, symmetric contour plots have been found which are shown Fig 6. As magnetic parameter increases there originate a secondary flow and only 2-vortex solution has been found for the secondary flow. The two vortexes are of same strength but rotating in counter clockwise direction.

In Fig. 6, the axial flow is greater in magnitude than secondary flow and it varies a great deal with magnetic parameter. As a result the difference between two consecutive contours line of the axial flow have been taken different for different magnetic parameters. For high magnetic parameter, Dean number and low curvature, the axial flow is shifted towards the centre of the duct as a result almost all the fluid particles strength are week.

4.3 Dean number $(D_n) = 1000$ at Curvature $(\delta) = 0.5$

In Fig. 5 we obtained the steady solution curve for non-dimensional flux (κ) with the variation of magnetic parameter for $D_n = 1000$ and $\delta = 0.5$. And it is clear that the flux increases with the increase of magnetic parameter. But if the magnetic parameter increases incessantly the rate of change of flux is trifling. For each figure the total flow is found to decreases as the magnetic parameter increase. The highest flux is found at $\delta = 0.5$ and $M_g = 1000$.

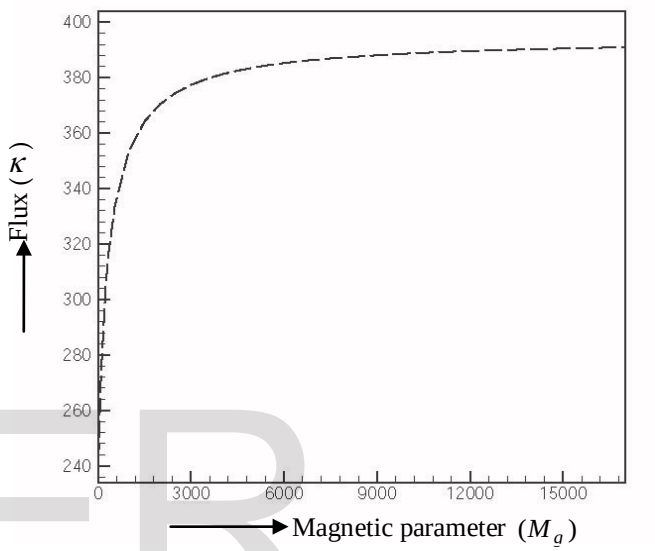

Fig. 5: Flux κ versus magnetic parameter M_g for Dean number $D_n = 1000$

In Fig. 7 the stream line, vector plots of the secondary flow and axial flow for different values of magnetic parameter at Dean Number $D_n = 1000$ have been shown at the first, second and third column respectively. The highest value of magnetic parameter, increment in axial velocity (Δw), increment in constant $\psi -$ lines ($\Delta\psi$) have been given on the right side of the above figure. For each figure the outer wall is to the right and the inner wall is to the left.

In case of axial flow behavior, the axial flow is also symmetric. The fluid particles are shifted towards the outer wall of the cross section and form a *low velocity band* inside the outer wall of the cross-section in Fig. 7. As magnetic parameter decreases the magnitude of the axial flow gets higher. The axial flow decreases with the increase of Magnetic parameter. Also the maximum axial flow is shifted to the centre from the wall of the cross section as Magnetic parameter increases. The vector plots of the secondary flow for $D_n = 1000$ and $\delta = 0.5$ has been shown in Fig 7. As the flow enters two vortexes flow is setup. The particles near the centre of cross-section gets out ward velocity, but the particles near the upper and lower boundary gets inward velocity

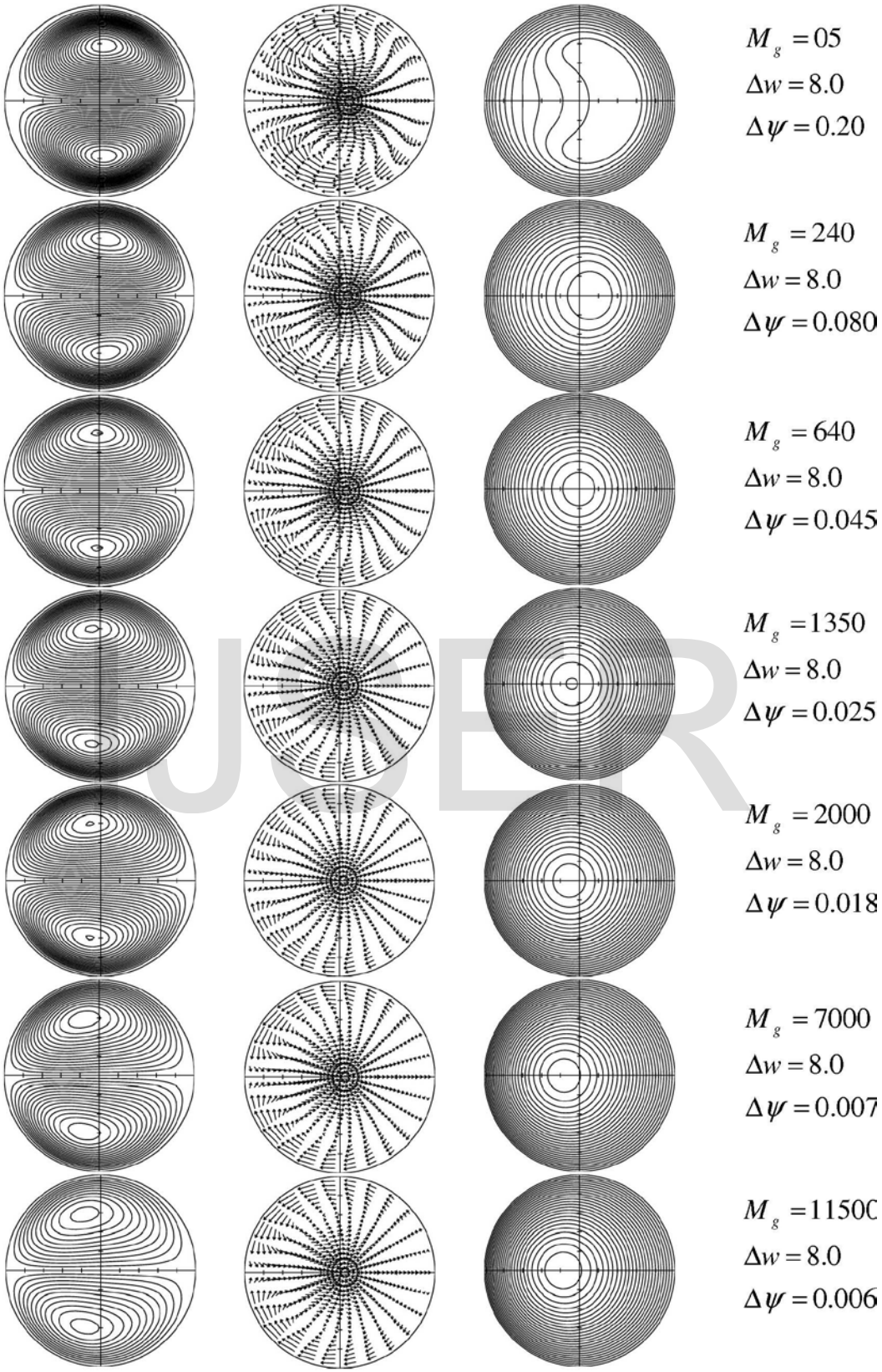

Fig. 6: The secondary flow, vector plots of the secondary flow and axial flow for different values of magnetic parameter at Dean Number $D_n = 800$

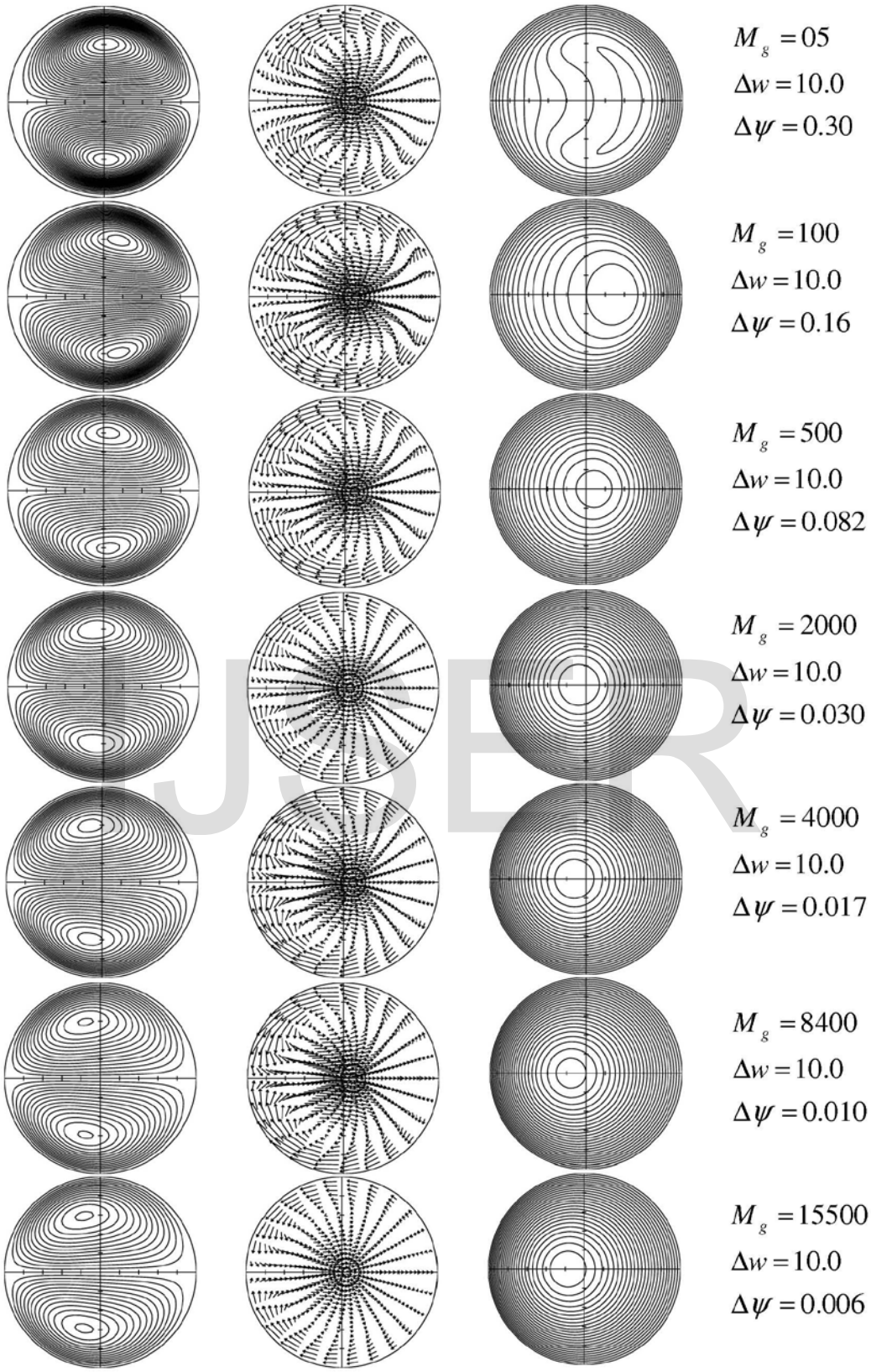

Fig. 7: The secondary flow, vector plots of the secondary flow and axial flow for different values of magnetic parameter at Dean Number $D_n = 1000$

4.4 Dean number $(D_n) = 2000$ at Curvature $(\delta) = 0.5$

In Fig. 8 we obtained the steady solution curve for non-dimensional flux (κ) with the variation of magnetic parameter for $D_n = 2000$ and $\delta = 0.5$. And it is clear that the flux increases with the increase of magnetic parameter. But if the magnetic parameter increases incessantly the rate of change of flux is trifling. For each figure the total flow is found to decreases as the magnetic parameter increase. The highest flux is found at $\delta = 0.5$ and $M_g = 30000$.

In Fig. 9 the stream line, vector plots of the secondary flow and axial flow for different values of magnetic parameter at Dean Number $D_n = 2000$ have been shown at the first, second and third column respectively. The highest value of magnetic parameter, increment in axial velocity (Δw), increment in constant ψ – lines ($\Delta\psi$) have been given on the right side. For each figure the outer wall is to the right and the inner wall is to the left.

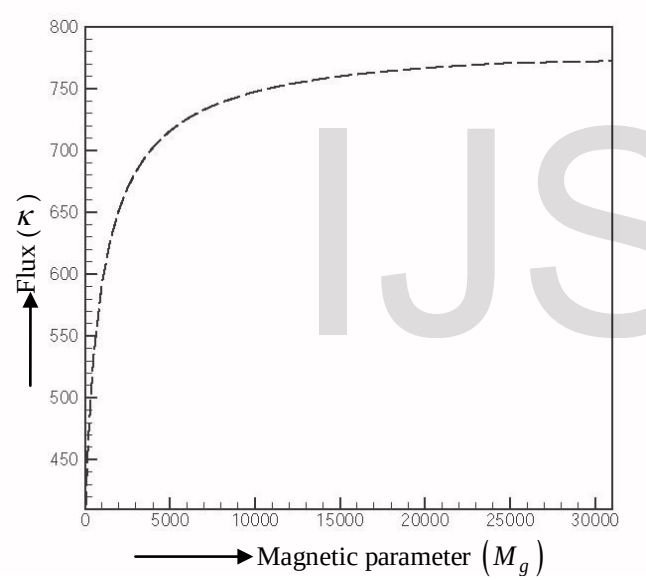

For $M_g > 30000$ and $\delta = 0.5$ convergence criteria is very poor and as a result no stable solution is found beyond this region. The stable solution zone initially increases with the increase of curvature. The largest magnetic parameter to give stable solution as well as an extra circular zone is $M_g = 25000$ for $\delta = 0.2$. It is clear that the fluid motion begins with two-vortex solution of the secondary flow as shown in stream line plots which stretches into the interior of the duct and the number of vortex that appeared of course depends on the Dean number (D_n) as well as magnetic parameter (M_g) which has been shown in Fig. 9 in the range $20 \le M_g \le 30000$. In the case of axial flow almost all the fluid particle is shifted to the centre from the wall of the cross section as Magnetic parameter increases.

At $M_g = 500$ and $D_n = 2000$ axial flow contours are nearly circular and are eccentric with the centers shifted towards the outer wall of the tube duct. At $M_g = 25000$ a strong magnetic field is found to confine the secondary flow streamlines to a thin layer near the tube wall. The secondary flow rate in the near wall boundary is increased by the magnetic field.

The contour plots of the axial velocity has been shown in Fig. 9 for magnetic parameter $M_g = 20$, 500, 1500, 1800, 3000, 5000, 7000, 11000 respectively for $D_n = 2000$ at $\delta = 0.5$. The axial flow is symmetric about the plane passing through the centre of cross section in the presence of magnetic field. As the flow enters the duct boundary layer begins to develop. Boundary layer near the inner wall develops faster than that at the outer wall. Just after the entrance, the axial velocity of the particle in the inner half is lower for small curvature. But as the flow precedes downstream the particles in outer half attains higher velocity.

At last, due to the effect of magnetic field a ***bracelet*** has been originates from the right corner of the duct and expands at $M_g = 7000$. This bracelet gradually increases with the increase of magnetic parameter and shifted to the centre. At $M_g = 5000$ the bracelet finally dropped to the centre and the bracelet also expand at magnetic parameter $M_g = 2000$

In the case, of vector plots of secondary flow a clock wise rotating vortex is set up after the entrance at $M_g = 20$. Also an anti–clock wise rotating vortex originates from the top and expands. On the other hand the secondary velocity of the particles around the center of cross–section decreases starting from the particles above the centre to the particles below the centre. Finally two vortex flow is found where the upper vortex is rotating anti–clock wise and the lower vortex is rotating clock wise, where the strength of the two vortices are almost same.

5 Conclusions

Studies on various aspects of the curvature as well as magnetic parameter have been made and revealed many physically interesting characteristics of the flows. The well constructed mathematical approaches numerically have been adopted to analyze the equations.

The flows were considered into two configurations, one is the flow in circular cross sectional duct with the variations of curvature and the other is circular cross sectional duct with high magnetic parameter. In this dissertation, steady solutions have been obtained by using the spectral method as a main numerical tool where Chebyshev polynomials and Fourier series have

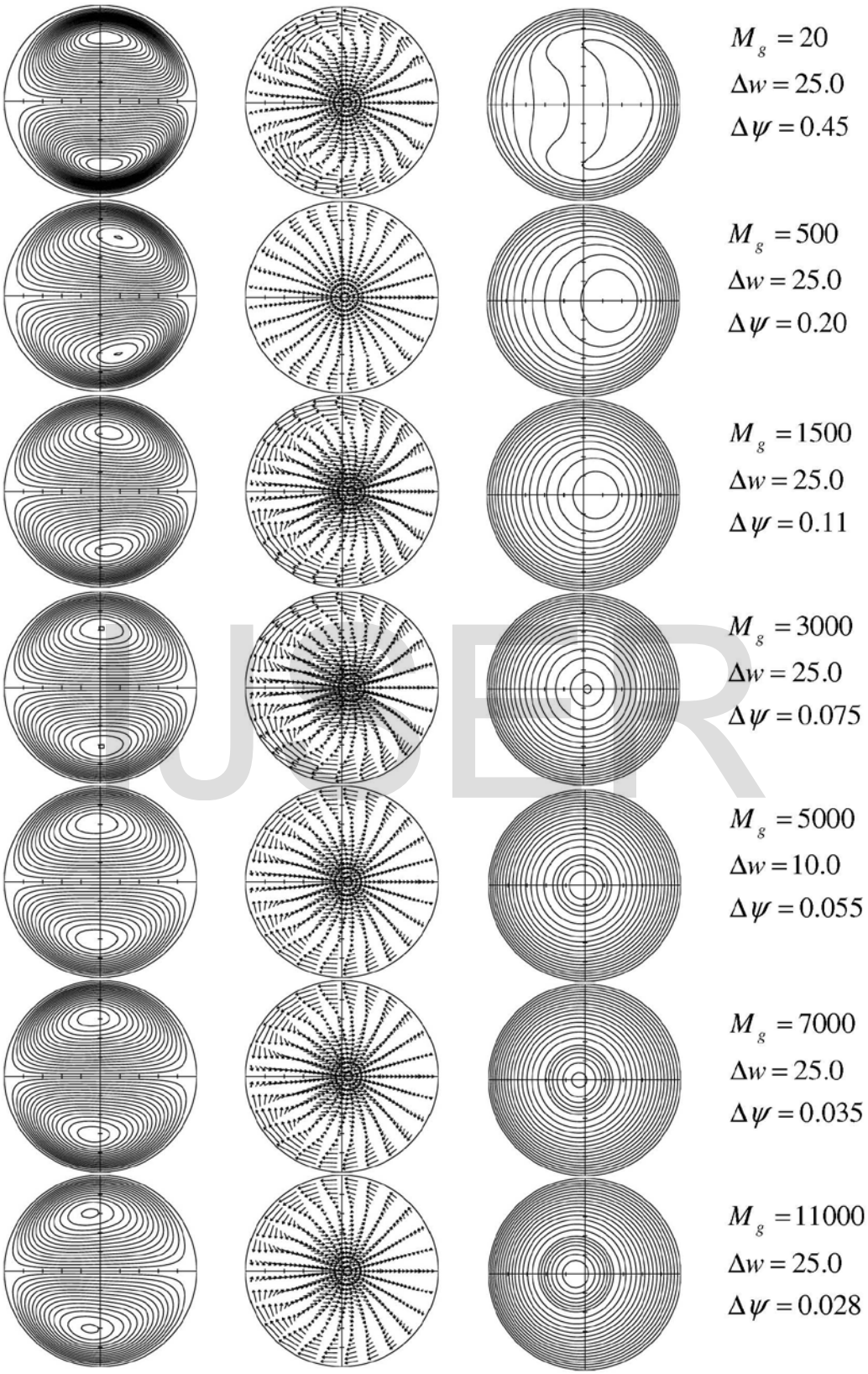

Fig. 9: The secondary flow, vector plots of the secondary flow and axial flow for different values of magnetic parameter at Dean Number $D_n = 2000$

been used in the radial and circumferential direction respectively.

The results obtained for each of the flows have been discussed and analyzed in the respective sections in detail. Since no experimental as well as numerical results of the corresponding studies are available. Therefore comparison of our results could not be made with experimental as well as numerical results.

However, qualitative agreements of our results with other numerical result are very good. From the point of the method of analyses and from the trends of the results obtained, it is well recommended that the present study can be extended to the other flows which are interesting to the engineers as well as to the theoreticians dealing with flow in curved duct. It is also interesting to carry out the experiment and compare the results with those of present study.

According to the present results, we can draw the following concluding remarks:

1. As Dean number as well as magnetic parameter increases there originate a symmetric contour plot and only 2-vortex solution has been found for the secondary flow. 2. The two vortexes are of same strength but rotating in counter clockwise direction.

3. The strength of the vortices is shifted to the outer half from the inner half with the increase of magnetic parameter, Dean number and curvature. As a result the difference between two consecutive contours line of the axial flow have been taken different for different magnetic parameters.

4. For high magnetic parameter, Dean number and low curvature, the axial flow is shifted towards the centre of the duct as a result almost all the fluid particles strength are week.

5. And finally due to the combined effect of the magnetic field and Dean number a ***bracelet*** has been originates from the right corner of the duct and expands for high Dean number and curvature.

6. For low magnetic parameter, contours are nearly circular. The effect of strong transverse magnetic field is to enhance the compression of fluid toward the outer wall. A strong magnetic field is found to confine the secondary flow streamlines to the duct wall. There are no drastic changes in the flow patterns except the quantitative differences.

REFERENCES

[1] Cheng, K. C. and Akiyama, M., (1970), Laminar forced convective hea transfer in curved rectangular channels, *International Journal of heat and mass transfer*, **Vol. 13**, pp. 471-490.

[2] Cheng, K. C., Lin, R. and Ou, J. W., (1975), Graetz problem in curved square channels, *Trans. ASME Journal of heat transfer*, **Vol. 97**, pp. 244-248.

[3] Cuming, H. G., (1952), The secondary flow in curved pipes, *Aeronautic Research Council Report, Mem*. **No. 2880**.

[4] Daskopoulos, P. and Lenhoff, A. M., (1989), Flow in curved ducts: bi furcation structure for stationary ducts, *Journal of Fluid Mechanics*, **Vol. 203**, pp. 125-148.

[5] Dean, W. R., (1927), Note on the motion of fluid in a curved pipe, Phil osophical magazine and Journal of Science, **4(20)**, pp. 208-223.

[6] Dennis, S. C. R. and Ng, M., (1982), Dual solutions for steady laminar flow through a curved tube, *Quarterly Journal of Mechanics and Applied Mathematics*, **Vol. 35**, pp.305-324.

[7] Dennis, S. C. R. and Ng, M., (1982), Dual solutions for steady laminar flow through a curved tube, *Quarterly Journal of Mechanics and Applied Mathematics*, **Vol. 35**, pp.305-324.

[8] De Vriend, H. J., (1981), Velocity redistribution in curved rectangular channels, *Journal of Fluid Mechanics*, **Vol. 107**, pp.423-439.

[9] Ghia, K. N. and Sokhey, J. S., (1977), Laminar incompressible Viscous Flow in Curved Ducts of Rectangular cross-section, *Trans. ASME, Journal of Fluids Engineering*, **Vol. 99**, pp.640-648.

[10] Ito, H., (1951), Theory on laminar flows through curved pipes of ellip tic and rectangular cross-section, The report of the institute of high speed Mechanics, Tohoku University, Sendai, Japan, **Vol. 1**, pp. 1-16.

[11] Joseph, B., Smith, E. P. and Adler, R. J., (1975), Numerical treatment of laminar flow in Helically Coiled tubes of square cross-section, *AIChE Journal*, **Vol. 21**, pp. 965-979.

[12] Masliyah, J. H., (1980), On laminar flow in curved semicircular ducts, *Journal of Fluid Mechanics*, **Vol. 99**, pp. 469-479.

[13] McConalogue, D. G. and Srivastava, R. S., (1968), Motion of a fluid in curved tube, *Proceeding of Royal Society of London Series A*, **Vol. 307**, pp. 37-53.

[14] Nandakumar, K. and Masliyah, J. H., (1982), Bifurcation in steady laminar flow through curved tube, *Quarterly Journal of Mechanics and Applied Mathematics*, **Vol. 119**, pp. 475-490.

[15] Shanthini, W. and Nandakumar, K., (1986), Bifurcation phenomena of generalized Newtonian fluids in curved rectangular ducts, *Journal of Non-Newtonian Fluid Mechanics*, **Vol. 22**, pp. 35-60.

[16] Winters, K. H., (1987), A bifurcation study of laminar flow in a curved tube of rectangular cross-section, *Journal of Fluid Mechanics*, **Vol. 180**, pp. 343-369.

[17] Yana se, S., Goto, N. and Yamamoto, K., (1989), Dual solutions of the flow through a curved tube, *Fluid Dynamics Research*, **Vol. 5**, pp. 191-201.